Measure of Horizontal Turbulence Intensity within Turbine Wakes using Ground-Based Doppler Lidar from the 2011 Crop Wind Energy Experiment (CWEX-11)

JAMES W. CAYER III
Mentors: Drs. Gene Takle and Dan Rajewski

Abstract

The wakes created by wind turbines have adverse effects on the conditions downwind of the flow. Two variables that can be measured to show the changes in these conditions is horizontal turbulence intensity and thermal stability. There is a lack of research conducted in the area of wake interactions on onshore utility-scale wind farms, making it important to understand the effects these turbines have on the small and large scale environment. Using data collected from meteorological surface flux stations and Ground-Based Doppler Lidars on an onshore utility-scale wind farm during CWEX-11 (2011 Crop/Wind-Energy Experiment), horizontal turbulence intensity and thermal stability were quantified and analyzed using statistical analysis and wind direction categories. Prior to calculating results, an increase in the difference between the downwind and upwind turbulence intensity was expected to be greatest in direct line of a turbine wake rather than along the edges of the wake for all types of stability (stable, unstable, neutral). This was confirmed to be true based on the statistical significance of the data. The highest increases tended to occur at or above turbine hub height (80m) for all types of stability, but also at 60 m for an unstable environment. This project focuses on understanding how turbine wakes influence changes in the flow field within a rotor depth (43-117m) at different wind directions and stability parameters.

1. Introduction

The current expansion of wind farms in the U.S. Midwest aims to support the federal objectives of improving production of electrical energy from renewable resources. Based on a report done by the U.S. Department of Energy (DOE) called the *20% Wind Energy by 2030*, they describe the steps needed to be taken in order to achieve 20% of the nation's electricity production using wind power by 2030 (U.S. DOE 2008). To achieve this large increase in production efficiently, there needs to be a better understanding of what impacts wind turbines and large wind farms have on the environment both at small and large scales. Wind turbines create perturbations in the flow by extracting a portion of the momentum from the wind for power, and generating turbulence behind the rotor-swept area of the turbine blades. This is a zone in the flow called a 'wake'. This turbine-induced turbulence in the wake may factor into underperformance of wind farms for turbines several km downstream from the initial line of turbines. Wakes are known to extend as far as 15 rotor diameters *D* downwind of the turbine (Meyers and Meneveau 2012), and the spread and extent of the wake before decay are related to three primary atmospheric variables (hub height speed, wind direction, and the temperature and wind speed gradients between the rotor and the surface). This is otherwise known as a measure of thermal stability as described in Rajewski et al. 2013a. and Barthelmie et al. 2013. According to Rhodes and Lundquist (2013), wake characteristics are determined by the inflow wind speed and elevation within the rotor disk, and normally create a region of reduced horizontal wind speed and increased turbulence downwind of the turbine.

Turbulence and other complex atmospheric events induced by turbulence (e.g. Low Level Jet) within wind farms could lead to adverse conditions of high speed and directional shear. This nighttime influence of intense but infrequent turbulence creates stresses on turbine blades and other components, which may reduce the effectiveness of a turbine or lead to malfunction or total failure several years before reaching the end of the manufacturer warranty (Kelley et al. 2001). Combinations of both wind tunnel (Chamaorro and Porté-Agel 2010) and numerical modeling (C.D. Markfort et al. 2013) techniques have been applied to explore patterns of turbulence within the wake of a single turbine or several lines of turbines. Many of these studies however, demonstrate simplified conditions of a homogenous inflow field with carefully tunable parameters (e.g. strength of wind speed). There are very few sets of field experiments in which these high resolution simulations of wind tunnel or computerized flow can be validated.

Field measurements of turbulence from utility-scale wind farm have been conducted in offshore locations and only recently are similar experiments occurring for land-locked wind farms, particularly over the Central U.S. agricultural landscapes. The Crop Wind Energy Experiment of 2010 and 2011 (CWEX-10/11) featured a combination of both surface and wind profiling measurements upwind and downwind of a leading line of turbines within a wind farm to detect turbine wake impacts on both crop surface fluxes and the wind and turbulence profile in the lowest 200m above the surface. Also during CWEX-11, Rhodes and Lundquist (2013) analyzed differences in turbulence intensity upwind and

downwind of a line of a few turbines to characterize the turbulence in the wake.

The purpose of this study is to expand upon their previous analysis and determine if and how atmospheric thermal stability influences the wake turbulence intensity. Before describing the instrumentation and methods I will quantify what is meant by turbulence intensity and provide the reader with previous findings from wake turbine wake modeling and field experiments.

2. Literature review

Turbulence intensity (i.e. kinetic energy of perturbations) I (%) takes the velocity fluctuations (i.e. variance) within a given layer to characterize stability, and is used as a mathematical representation of the overall level of turbulence in relation to the mean wind speed $\overline{U}$ (m/s) (Lundquist and Wharton 2011). An example of an early wind tunnel study that looks at turbulence intensity was done by A. Papaconstantinou and G. Bergeles (1988). This experiment uses wind tunnel hot-wire measurements of the time-averaged flowfield within a three bladed rotor that measured 2.43 m in diameter. From these measurements, they were able to calculate mean the turbulence intensity using statistical methods. Following these calculations, they were able to conclude turbulence intensity levels remain small upstream of the rotor, but notice a large increase in these levels directly downstream of the rotor. These increases were greatest along the tip and the root of the rotor blades, and persisted much further downwind than any other part along the blade. This was quantified by using the blade diameter (*D)* as a distance measurement and showed that at *x=D/60* and *x=D/4*, the general amount of turbulence has decreased by 60% along all parts of the blade besides the tip and root. The tip and root only experienced a 20% decrease. Chamaorro and Porté-Agel (2010) are researchers who have done recent work with wind tunnel studies on wind turbine wakes. The study that pertains to this project is a simulation of a wind turbine within boundary layer flow in a neutral and stratified stable environment. In a stratified stable environment, colder and denser air parcels are found below warmer and less dense air parcels, thus inhibiting any vertical motion or overturning of air parcels. From this study, they were able to compute the statistics of turbulence variables, in particular, turbulence intensity. Taking the measurement of each wind component and the temperature at certain levels, they were able to come to 2 types of conclusions for the turbulence intensity in a neutral and stratified stable environment. In a stratified stable environment, they found the turbulence intensity is strongest above hub height, and a distance 3 to 6 blade diameters *D* downwind. This makes sense because less dense air parcels exist above the stable surface boundary layer, and are moving at much higher speeds at this level allowing turbulence to be induced by the rotation of the turbine blades and the vertical shear. In a neutral environment, the strongest turbulence intensity is above the hub height as well, but the distance and magnitude of turbulence intensity is slightly less. This case is different from a stratified stable environment because the wind speed is more uniform from the surface to the turbine layer, and less lateral shear exists. Another wind tunnel study done by C.D. Markfort et al. (2012), looked at turbine wakes within a simulated convective boundary layer. Upon calculating turbulence intensity based on the measurements done using the same instruments as the previous study, they concluded that the peaks occur just above and below the hub height at distances roughly 1.5 to 2 blade diameters *D* downwind of the flow. A brief peak also occurs at the bottom tip of the blades due to the convective mixing that occurs at the surface, thus enhancing the turbulence intensity.

Other early studies on wind turbine wakes use numerical models, such as the one created by J.F. Ainslie (1988). Here, he compared variables like the ambient turbulence intensity within the wake flowfield using the numerical solution of set differential equations. These equations were only simplifications of what might be occurring in a real environment behind a single wind turbine, and cannot be applied to current studies involving such variables however. Modern studies can use numerical models to create flow simulations such as the one done by C.D. Markfort et al. (2013). This study was ultimately comparing the similarities and differences between staggered turbines and aligned turbines within wind farms using measurements from variables like turbulence intensity. Their results show the strongest area of turbulence intensity is at the top tip of the turbine blades for both staggered and aligned turbines. There was a second region of strong turbulence intensity at the bottom tip of the blades, with areas of weak turbulence intensity existing at hub height and at the surface. Overall, staggered wind farms showed less turbulence intensity than aligned wind farms, because the transfer of momentum within the flow is more efficient and power output is better by roughly 10% (C.D. Markfort et al. 2013). Because this paper is using data from CWEX-11 where air flow is induced by a line of turbines rather than a staggered wind farm, it can be expected there will be areas of

increased turbulence intensity based on the results of this flow simulation model. Empirical models, similar to the models done by C.D. Markfort et al. (2013), are currently the best models available to help forecast and show turbulence intensity within a wind farm, because they are created based on previous observed data. The problem with these models however, is their sensitivity to estimating variables, making it hard to use for varied wind farm configurations. No theoretical models have yet to be created as well, with a lack of data to support such projects.

Early field studies were the best way to begin deciphering the types of flow characteristics created by turbine wakes. For instance, a field study done by U. Högström et al. (1987), took measurements behind a 2 MW wind turbine using a high resolution sodar and tala kites from the surface to 100 m. From these field measurements, a number of key variables were analyzed including turbulence intensity. Part of the analysis compared the difference between when the blades were turning and not turning, and how eliminating the influence of the wake can change the overall flowfield. For all of the wake cases, they see an increase in turbulence compared to an undisturbed case. Another aspect of the study showed turbulent fluctuations from a wake measured at a fixed position (via sodar) has contributions from several mechanisms. These mechanisms include ambient turbulence of a scale smaller than the width of the wake, the meandering of a wake, shear within the wake that creates turbulence, turbulence directly caused by the turbine, and the vertical temperature gradient that can create stratification and increased turbulence in the wake (U. Högström et al. 1987).

Magnusson and Smedman (1998) performed an experiment on a small scale wind farm consisting of four 180 kW turbines with a 35 m hub height. Using two meteorological masts with attached instruments measuring wind speed and direction at 8 heights, and temperature at 5 heights, they were able to plot vertical profiles of variables including turbulence intensity and velocity deficit (i.e. horizontal wind shear). Velocity deficit is another variable used in field studies to describe the changes in turbulence intensity, and will be used briefly in this paper to explain any correlation between the two variables within the data. The velocity deficit is defined as $U_{up} - U_{dn}$ where U_{up} is the upwind velocity and U_{dn} is the downwind velocity (Magnusson and Smedman 1998). It was found that the velocity deficit decreased at lower wind speeds, but increased at higher wind speeds because a turbine is running more efficiently at lower wind speeds despite the production of less power. This is directly related to stability, as more stable conditions result in higher wind speeds aloft and higher velocity deficits, whereas unstable conditions result in lower wind speeds aloft and lower velocity deficits. Using the calculated turbulence intensity, they were able to conclude that the travel time (t_0) of turbine wakes are inversely proportional to turbulence intensity and the frequency of the blades' rotation. This means the less time it takes for the flow to reach the turbines, the stronger the turbulence intensity will be in the wake as the blades rotate faster. Because this project was done on a small scale wind farm with staggered turbines rather than aligned turbines, the data from CWEX-11, which was also used in the field study done by Lundquist and Rhodes (2013), will prove to be the most vital. In their study, the main focus is to look at the effects of turbine wakes based on Ground-Based Doppler Lidar measurements at the instruments' allotted vertical range (40 m to 220 m).

The importance of using Ground-Based Doppler Lidars for these types of measurements within a wind farm is their ability to capture data at much higher heights than any type of instrument mounted to a meteorological tower. Typically, turbine rotor disks extend from 40 m to 120 m, which is much taller than most meteorological towers, and gaining funding or permission to erect such towers of this height can be difficult. Therefore, Ground-Based Doppler Lidars are a viable option to breaking the barrier between surface tower measurements, and turbine layer measurements. The overall performance of taking measurements using Ground-Based Doppler Lidars has been tested by Aitken et al. 2012, and the results of this field study done in Iowa and Colorado show that the four most significant factors that influence the lidar performance are aerosol backscatter, atmospheric refractive turbulence, humidity, and precipitation. Both humidity and precipitation have negative effects on the performance of the lidar, as the speed of the water droplets in the air are measured instead of aerosols, thus creating errors in vertical wind speed. Therefore, data that includes precipitation or high humidity will have a strong bias, and was not included in the data for this paper. Using data from CWEX-11 derived from the two lidars that measured the wind-speed components (u,v,w), wind direction, wind-speed variance (σ_u, σ_v, σ_w) at specific heights, Rhodes and Lundquist (2013) were able to calculate a number of variables including wind shear, directional shear, horizontal turbulence intensity (I_U), vertical turbulence intensity (I_W), and a form of turbulent kinetic energy (*TKE*) for

their study. Based on the differences of the upwind lidar (WC-68) vs. the downwind lidar (WC-48), turbulence intensity is greater during the day than at night for all periods (Lundquist and Rhodes 2013). This is due to the natural reduction of wind speed during the day than at night. Using a stable nighttime case study from 2100 LST on 16 July 2011 to 0700 LST on 17 July 2011, there was a full analysis done on the difference in turbulence intensity between the two lidars. This case recorded hub height wind speeds averaging 7-9 m s^{-1} contained in mainly southerly flow. As stated earlier, the turbulence intensity is less during the night than during the day, but there is still an area of strong turbulence intensity above the rotor disk. This coincides with previous conclusions in wind tunnel studies (Chamorro and Porté-Agel 2010). The turbulence intensity increased downwind during sunrise and continued to spread throughout the rotor disk area. Based on each type of study done on turbine wakes and their relationship to turbulence intensity, this paper seeks to expand upon these results and focus mainly on thermal stability and how the turbulence intensity can increase downwind of the turbines from within or outside certain wake windows.

3. Experimental Methods

3.1 Site Layout

To ensure proper analysis of the results for this project, there needs to be a review of the structure of the site from which the data was extracted. According to Rajewski et al. (2013a), the CWEX-10and CWEX-11 project took place within a 200-turbine (1.5 MW rated power) wind farm located in the Central Iowa during the months of June-August. The turbines stand with hub heights measuring 80 m, and rotor diameters of 74 m. These turbines have a rated wind speed of 12 m/s, and turn on with speeds greater than 3 m/s and turn off with speeds greater than 25 m/s. The land on the wind farm is relatively flat, with a slope that is less than 0.5° from southwest to northeast. The crops that are contained within the area of the wind farm are a mix of corn and soybeans. Measurements taken by Ground-Based Doppler Lidars (WC-68, WC-49) and ten surface flux stations (ISU 1-2, NCAR 1-4, NALE 1-4), were all located on the southwest edge of the wind farm. As shown in Fig. 1, the B turbine line (B1-B6) is the general area being measured during CWEX-11and CWEX-10, and are spaced approximately 3.8 rotor diameters or 282 m between each other. Specifically, the wake region from the B3 turbine is going to be the main area of focus for this study because it is in line with WC-49 and WC-68. WC-49 is located 250 m (3.4*D*) north of turbine B3 and WC-68 is located 165 m (2.2*D*) south of turbine B3. The data from WC-49 and WC-68 are converted to 10-min averages from the raw measurements taken each second at 20 m intervals from 40 m to 220 m.

3.2 Wind Direction Sort

The wind direction window (150-200 degrees) used for this project is based on the 80 m wind direction measurements taken from WC-68 because the airflow is yet to be perturbed by the turbines. With this window, the entire width of the B3 wake can be captured by WC-49, as well as any measurable differences in horizontal turbulence intensity felt along the edges of the wake due to influences from the B2 and B4 wake. One reason for using this direction window is based on the climatology of the area's wind directions during the mid to late summer months. In Fig. 2 a) and b), wind roses are plotted using the wind direction data from NCAR1 and WC68 during the collection period of CWEX-11. The images show a predominately south direction throughout the experiment, making this favorable for capturing wakes from the B line of turbines.

a)

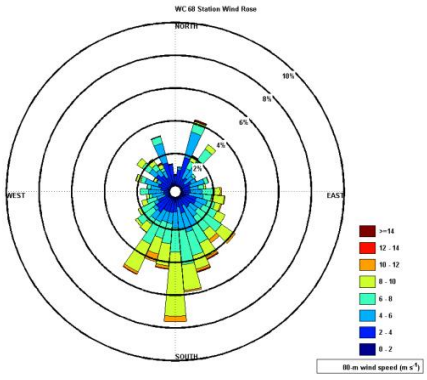

b)

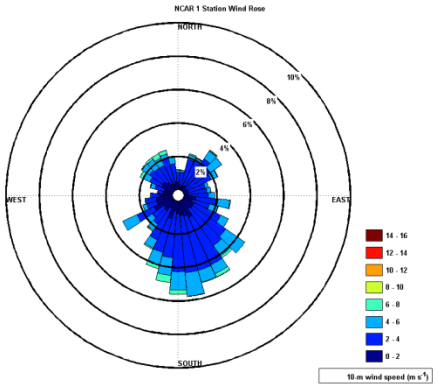

Fig. 2 a) and b) show Climatological 10-m wind rose of NCAR1 tower and 80-m wind rose of Upwind lidar (WC68) (CWEX-11)

Besides looking at the climatology of wind directions, all the data involving wakes from B1-B4were placed into separate bins based on the range of wind directions for each wake, daytime and nighttime cases, and when turbines were operational. The West bin was used as a null case. All cases where the turbines B1-B4 are off are placed in their own separate bin for each stability parameter (daytime unstable, daytime neutral, and nighttime stable). The sorting of these variables were the next key steps in the process of designing the methodology for the project. The individual summation of daytime unstable, daytime neutral and stable nighttime cases, coupled with the respective wake regions captured by WC-49 and WC-68, showed areas clearly lacking more data than others. Overall, the area with the most data available was the wake region within and just outside B3 (B23G, B34G). Table 1 gives the best representation of why directional bins were used to organize the data to check the availability of each stability classification. As stated in the Literature Review, data containing any precipitation was separated from this analysis due to the strong bias it creates in Ground-Based Doppler Lidar measurements. Transitional periods between day and night were also separated from the data, using nighttime periods when the net radiation was $\leq$ 0 W/m^2 and daytime periods when net radiation was $\geq$ 300 W/m^2 (taken from Rajewski et al. 2013b).

Turbine Wake	Classification of Wake Region (°)	Nighttime Stable: # of Data Points	Daytime Neutral: # of Data Points	Daytime Unstable: # of Data Points
B12 Combo	224.4-266.3 (WSW)	165	104	10
B23G	193.6-211.5 (SW)	141	43	8
B3	166.4-193.6 (S)	248	136	45
B34G	147.7-166.4 (SE)	58	77	54
West	266.3-273 (W)	37	2	3
Off	Turbines B1-B4	105	1	126
On	Turbines B1-B4	612	360	117

Table 1: separation of turbine wake regions B12 combo, B23 gapped flow, B3, B34 gapped flow, West, and data available for project's stability classifications with turbines on or off.

As the table shows, the wind direction from the B3 turbine wake has the most data available, with the flow between B3 and B2 (B23G) and between B3 and B-4 (B34G) having the second most. Another reason for choosing 150 to 200 degrees as the range of wind directions is to capture a smaller window of differences in horizontal turbulence intensity. To better display the range of the various directional bin categories and how they will be seen by the downwind lidar (WC49), Fig. 3 uses a zoomed in version of Fig. 1with the colors corresponding to Table 1. The wake window from the B4 turbine was not used in the sorting process because its flowfield has influences from a line of turbines southeast of it.

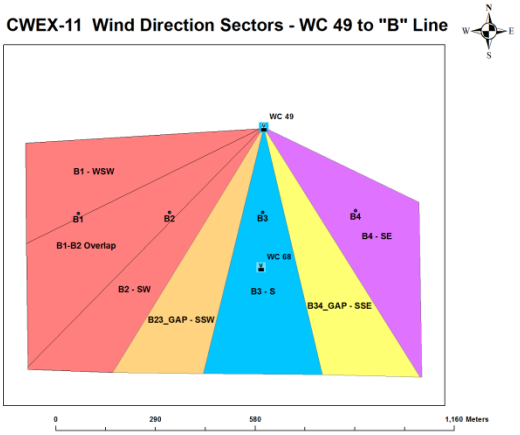

Fig 3: B1 – B4 turbines, downwind lidar (WC49), and upwind lidar (WC68), with colors corresponding to each directional bin category.

In the data section, all the wake bin categories will be paired with their respective stability classifications and compared to the stability classifications within the smaller wake window.

3.3 Stability Parameters

Stability classifications were done based on thermal stability (z/L_o) of NCAR1, where z is the height of the sonic anemometer (4.5 m) and L_o is the Obukhov length. The Obukhov length is defined by Stull (1988) as

$$L_0 = \frac{-\overline{\theta_v} u_*^3}{kg(w'\theta'_v)_s}, \qquad (1)$$

where k is von Karman's constant (0.4), u_*^3 is the friction velocity, $\overline{\theta_v}$ is the surface virtual potential temperature, and $\overline{(w'\theta'_v)_s}$ is the surface moist sensible heat flux. For an unstable, neutral and stable atmosphere, $z/L_o < -0.05$, $-0.05 < z/L_o < 0.05$, and $z/L_o > 0.05$ respectively. These are the ranges used for defining the stability for all periods in the data. Each wake category was plotted with the stability range of the difference in horizontal turbulence intensity in MATLAB with respect to the means and 95% confidence intervals. This was done to test the variability of the difference in horizontal turbulence intensity within the range of stability for a given wake.

3.4 Horizontal Turbulence Intensity

From the 10-min averaged data of the two horizontal wind velocity components (u, v) and the variances of these variables (σ_u, σ_v), the horizontal turbulence intensity I_U can be calculated as:

$$I_U = \frac{\sqrt{\sigma_u^2 + \sigma_v^2}}{U} \qquad (2)$$

where U is the mean horizontal wind speed at a level the velocities are observed (Stull 1988). In this case, the levels will be from (40 m to 120 m). For determining I_U of the downwind and upwind locations, U will be taken from WC-68 because it will be an unbiased measurement with no influences from turbine wakes. Upon calculating I_U from WC-68 and WC-49, the difference in magnitude between the two quantities will be the key component to the analysis of this data. The difference ΔI_U will be defined as:

$$\Delta I_U = I_{U_{WC-49}} - I_{U_{WC-68}} \qquad (3)$$

which is a unitless quantity (%). Understanding what causes larger or smaller differences in I_U within different portions of a wake will be discussed in the analysis of the data. To show how different wakes create a difference in I_U, the means and 95% confidence intervals were plotted using MATLAB within the turbine rotor depth. A nonparametric two sample wilcoxon method t-test was also done for each stability case comparing the centerline wake (B3) versus turbines being off, flow along the edges of the wake (B23G and B34G), and the combination of wakes from B1 and B2. A test was also done to compare the edges of the wake (B23G vs. B34G). The t-test was done from 60 m to 100 m because previous studies on turbulence intensity show the strongest increases to occur within this region of the rotor depth.

4. Results

4.1 Difference in Horizontal Turbulence Intensity for Daytime Unstable Conditions

In Fig. 4a, a mean and 95% confidence interval for ΔI_U is shown for the daytime unstable case from each directional bin category. In Fig. 4b, a mean and 95% confidence interval for ΔI_U is shown for the daytime unstable case from 150 to 200 degrees across the depth of the turbine rotor disk. Within figures 4 a) and b) there is a large variability in ΔI_U. This is expected with an unstable environment, as lateral winds are not as strong (confirmed by more data for when turbines were off). The largest recorded difference for the assorted directional bins was within the wake from the B3 turbine at 3%. The largest recorded difference in the smaller directional window was from 180 degrees at 2.6%. These larger values occurred at 60, 80, and 100 m. This supports the hypothesis of increased ΔI_U within the centerline of wake to be the greatest. What was not expected however, were the negative values in ΔI_U as you moved towards the edges of the wake. This was especially evident at B23G, B12C, 150, 190, and 200

degrees. When looking at Table 2, none of the comparisons made between the directional bin categories proved to be statistically significant (p-values<0.05), but showed relatively large values (6-8%) in the mean ordered differences ($\overline{\Delta I_U}$) because of the variability of the flow pattern within different wakes during the day. If there was more data allotted for this period, the pattern would prove to be much clearer.

4.2 Difference in Horizontal Turbulence Intensity for Daytime Neutral Conditions

In Fig. 5a and b, we took the daytime neutral case and made a similar plot of ΔI_U as shown in Fig. 5a and b. Here, values appear to be slightly lower in 5a than they are in 4a, which is likely due to the natural decrease in turbulence within a neutral environment compared to an unstable environment. The variability of each category is also much less than the unstable case. The highest recorded difference in turbulence intensity in 5a was within the B3 turbine wake at 2%. This is the same turbine wake that had the largest ΔI_U as the unstable case, thus supporting the hypothesis of the centerline of wake to contain the most ΔI_U. In 5b, we see a slightly different result from the unstable case, as ΔI_U tends to be the strongest at 170 degrees, with a value of 4.75% increase in horizontal turbulence intensity. A similarity to the unstable case is the negative values in ΔI_U, but only occurring at B23G and 200 degrees. In Table 3, there is statistical significance between the B3 turbine and B12 turbine combo at all three levels (bolded in red). Here, $\overline{\Delta I_U}$ is much smaller than the unstable case with values at 2%, but the p-values are under 0.05. This means that there is a statistically significant difference in horizontal turbulence intensity between the combinations of two wakes versus the centerline of a wake by a magnitude of 2%.

4.3 Difference in Horizontal Turbulence Intensity for Nighttime Stable Conditions

In Fig. 6a and b, the mean and 95% confidence interval of ΔI_U is displayed for the nighttime stable case. This is the case containing the most positive values for ΔI_U, having the highest differences occur above the rotor disk like the other cases. The values in 6a and b are relatively consistent with the other cases as well, mainly hovering between 0-4% increases. The highest ΔI_U is coming from the B3 turbine, resulting in an increase of horizontal turbulence intensity by 2.8%. This is the second highest recorded difference based on the directional bin categories for all three stability cases (day unstable is higher). This large value also confirms the hypothesis that all stability parameters will experience the highest ΔI_U in the centerline of a wake. In 6b, the highest increase in ΔI_U is along the edges of the wake by the B3 turbine at 170 and 190 degrees. The highest recorded increases were between 3 and 3.5% percent, at 80 m and 100 m. This case was also contained the most statistically significant comparisons as shown in Table 4 (in red). Although there were more statistically significant comparisons, the $\overline{\Delta I_U}$ stayed consistently around 2% like the neutral case. This is not a very large ordered difference, but it is enough to prove the increase in horizontal turbulence intensity downwind in the centerline of a wake is greater than the edges of a wake or the combination of 2 wakes.

5. Analysis and Interpretation

5.1 Horizontal Turbulence Intensity and Thermal Stability

After reviewing the preliminary results of this study, there are a few key points that were found to coincide with previous research on turbulence intensity. For instance, Rhodes and Lundquist (2013) found that the difference in turbulence intensity occurs mostly at the hub height (80 m) or slightly above it (100 m), during their nighttime stable case study. The difference was calculated the opposite way however, taking the upwind site minus the downwind site. This gave ΔI_U values as high as -25% with upwind wind speeds ranging from 8 to 10 m/s. This data was also used with 2 minute averages rather than 10 minute averages for their experiment, making fluctuations in turbulence intensity seem more severe, which is why the differences for this study are not as high. Lundquist and Rhodes (2013) also used a composite of the data rather than separating the values into specific wind directional bins like this current analysis has demonstrated. Based on wind tunnel studies done by Chamorro and Porté-Agel 2010, their results showed increases in turbulence intensity to be at and above the hub height, with the strongest turbulence intensity during a stratified stable environment. The result does not correlate with this study because the overall increase in turbulence intensity appears to be slightly stronger in a neutral environment compared to a stable environment. The difference from this study could be due to applying weakly stable conditions ($Z/L_0 \sim 0.25$) to the wind tunnel model, as compared to values in CWEX-11 where strongly stratified stable conditions occurred. When sorting the Nighttime stable conditions, there was a noticeably stronger thermal stability range of $0.05 < Z/L_0 < 32$. Nighttime conditions normally

showed significant upwind speed and directional shear between the surface and the top of the rotor (Rajewski et al. 2013 and Fig. 2 of this paper). Because of this speed and directional shear at night, wakes become disturbed and do not have a uniform expansion shape downwind of the turbine. Therefore, turbine generated σ_u and σ_v (2) are becoming "dampened" as the wake is moving downstream of the turbine, thus decreasing the amount of wake generated turbulence intensity. In a neutral environment however, there is not as much directional and speed shear, thus allowing a slightly higher increase in turbulence intensity compared to stable conditions. Comparing the results of the daytime unstable turbulence intensity with Markfort and Zhang (2012), who looked at this variable in a convective boundary layer, shows similarities with this study. For instance, the highest values of increased turbulence intensity they recorded were just below the hub height and just above the hub height. This coincides with the results of this study, as higher increases of turbulence intensity are mostly felt between 60-100 m. This is especially true in Fig. 4a, as the 60, 80, and 100 m layers all have roughly the same increase in turbulence intensity from the B3 wake. The reason for this homogeneity within the low levels and upper levels of the turbine layer is due to the turbulent mixing of the surface with the air aloft (Markfort and Zhang 2012). As seen in Table 2, $\overline{\Delta \boldsymbol{I_u}}$ is large for each comparison test. Even though these comparisons were not deemed to be statistically significant due to lack of data and large variations in values, the table still displays the strong increase in horizontal turbulence intensity that is created in an unstable environment.

6. Conclusions

Wind turbine wakes that are created by the rotation of the blades, greatly impact the flow field downwind of the turbine, and are normally combined with added turbulence intensity. Our results show this correlation, as we expanded upon the field study done by Lundquist and Rhodes (2013) using thermal stability as a classification. We also used wind direction bins to separate out the wakes from different sections of the B line of turbines. Overall, the analysis shows a positive increase in horizontal turbulence intensity with values between 0 to 5% (greatest values occur during daytime unstable conditions). Even though these values are not as large of an increase as shown from previous studies, it still poses the argument that there will be an increase in horizontal turbulence intensity as air passes through the turbine rotor depth. A better understanding of these wake interactions in different ranges of thermal stability with increases in turbulence intensity will have a profound impact on the ability to design turbines to withstand higher amounts of stress on the rotor blades. This will thus increase the efficiency of wind turbines, and increase power output. Additional research ideas include: measuring vertical turbulence intensity using a larger vertical cross section (surface to turbine layer), instead of just the turbine rotor depth.

Acknowledgements
I would like to thank Drs. Daniel Rajewski and Gene Takle for providing the guidance and data for this project, Dr. Julie Lundquist for providing the lidars that were part of the CWEX-11 project and important for this paper, and finally Russell Doorenbos for providing the images that display the area being studied within the wind farm.

References

Aitken, Matthew L., Michael E. Rhodes, Julie K. Lundquist, 2012: Performance of a Wind-Profiling Lidar in the Region of Wind Turbine Rotor Disks. *J. Atmos. Oceanic Technol.*, **29**, 347–355.

Barthelmie, R. J., Pryor, S.C., Frandsen, S.T., Hansen, K.S., Schepers, J.G., Rados, K., Schlez, W., Neubert, A., Jensen, L.E., and Neckelmann, S., 2010: Quantifying the impact of wind turbine wakes on power output at offshore wind farms. *J. Atmos. Oceanic Technol.*, **27,** 1302–1317, doi:10.1175/2010JTECHA1398.1.

Chamorro LP, Port´e-Agel F, 2010: Effects of thermal stability and imcoming boundary-layer flow characteristics on wind-turbine wakes: a wind tunnel study. *Boundary-Layer Meteorology*, doi: 10.1007/s10546-010-9512-1.

Kelley ND, Osgood RM, Bialasiewisz JT, Jakubowski A., 2001: Using wavelet analysis to assess turbulence/rotor interactions. *Wind Energy*, **3**, 121–134.

Magnusson M, Smedman AS, 1998: Air flow behind wind turbines. *Journal of Wind Engineering Industrial Aerodynamics*, **80,** 169-189.

Markfort CD, Zhang W, Port´e-Agel F, 2013: Turbulent flow and scalar transport through and over aligned and staggered wind farms. *Journal of Turbulence*, **33,** 1-36.

Markfort CD, Zhang W, Port´e-Agel F, 2012: Wind-turbine wakes in a convective boundary layer: a wind-tunnel study. *Boundary-Layer Meteorology*, **146,** 161–179.

Meyers, J., and C. Meneveau, 2012: Optimal turbine

spacing in fully developed wind farm boundary layers. *Wind Energy*, **15,** 305–317, doi:10.1002/we.469.

Rajewski, D.A., E.S. Takle, J.K. Lundquist, S.P. Oncley, J.H. Prueger, T.W. Horst, M.E. Rhodes, R. Pfeiffer, J.L. Hatfield, K.K. Spoth, and R.K. Doorenbos, 2013a: CWEX: Crop/Wind Energy Experiment: observations of surface-layer, boundary-layer and mesoscale interactions with a wind farm *Bull. Amer. Meteor. Soc.*, **94**,655-672. doi:10.1175/BAMS-D-11-00240.

Rajewski, D.A., E.S. Takle, J.K. Lundquist, J.H. Prueger, R.L. Pfeiffer, J.L. Hatfield, K.K. Spoth, and R.K. Doorenbos, 2013b: Changes in fluxes of heat, H_2O, and CO_2 caused by a large wind farm. Submitted to *Agric. For. Meteor*.

Rhodes ME, Lundquist JK, 2013: The effect of wind-turbine wakes on summertime US Midwest atmospheric wind profiles as observed with ground- based doppler lidar. *Boundary-Layer Meteorology*, doi: 10.1007/s10546-013-9834-x.

Stull, R., 1988: *An Introduction to Boundary Layer Meteorology.* Kluwer Academic Publishers, 666 pp.

U.S. DOE, 2008: 20% wind energy by 2030: Increasing wind energy's contribution to U.S. electricity supply. NREL Rep. TP-500-41869, DOE/GO-102008-2567, 248 pp. [Available online at www.nrel.gov/docs/fy08osti/41869.pdf.]

Wharton Sonia, Lundquist JK, 2011: Assessing atmospheric stability and its impacts on rotor-disk wind characteristics at an onshore wind farm. *Wind Energy*, doi: 10.1002/we.483.

Appendix

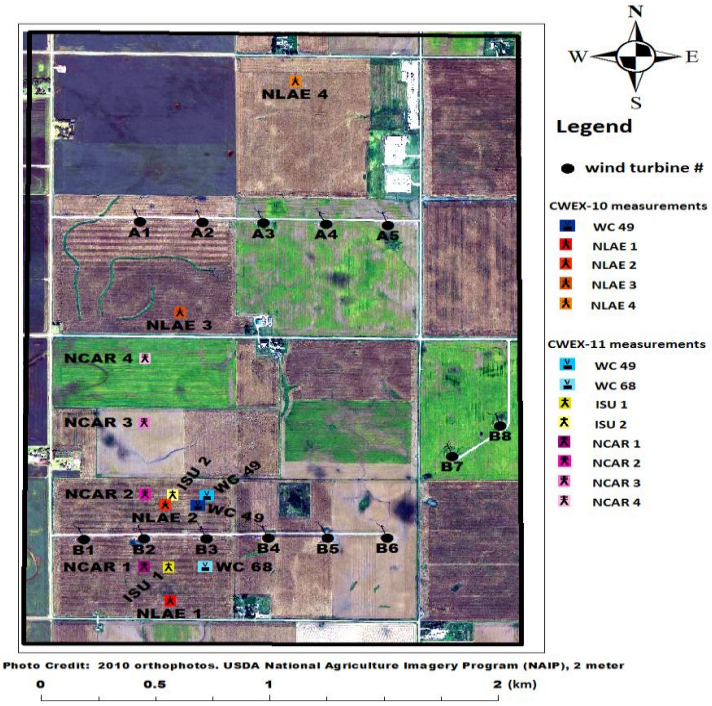

Fig. 1. As taken from Rajewski et al. (2013) with permission. Overhead view of the measurement locations for CWEX-10 and CWEX-11.

a)

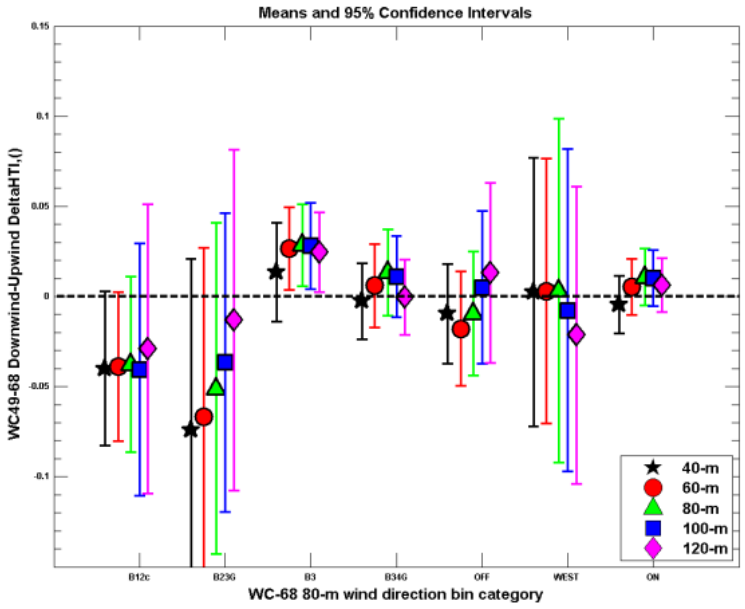

b)

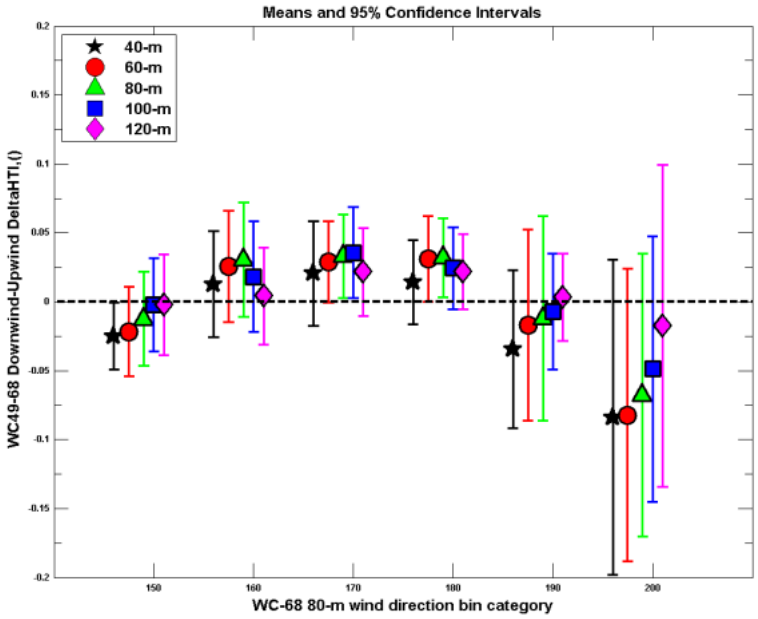

Fig. 4 a) and b) show means and 95% confidence intervals for ΔI_U based on wind direction categories for a daytime unstable case.

a)

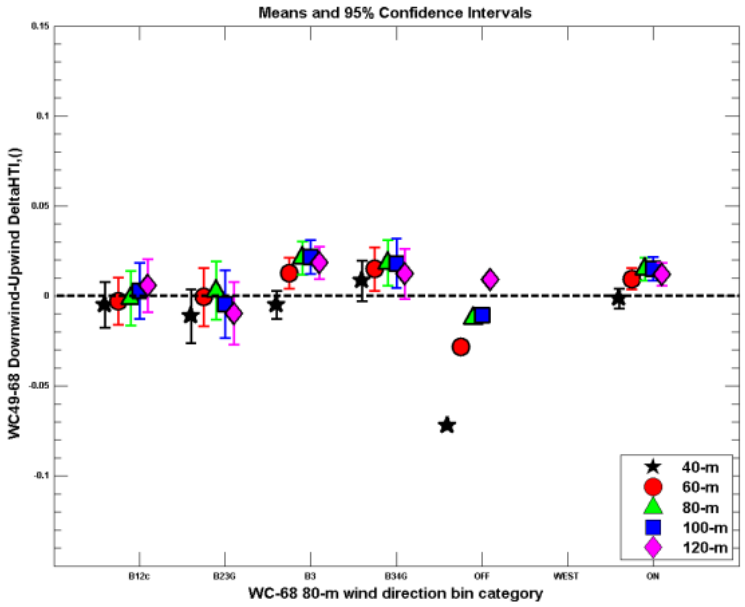

b)

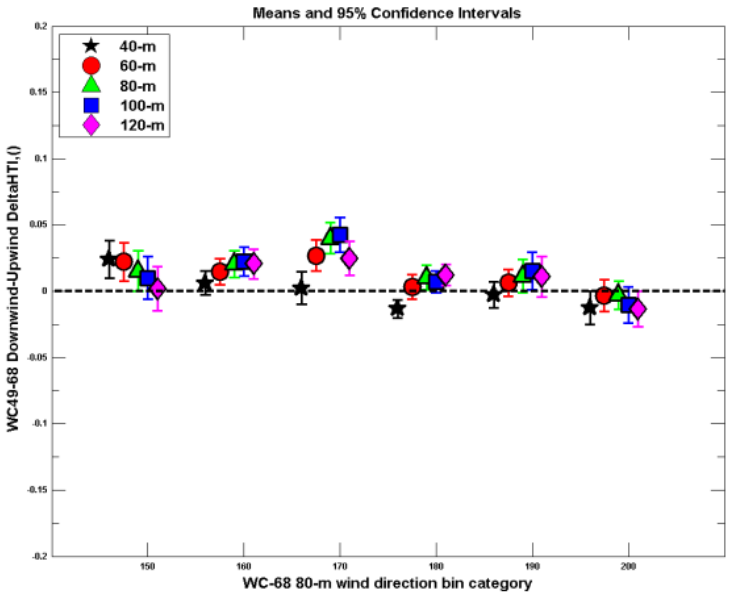

Fig. 5 a) and b) show means and 95% confidence intervals for ΔI_U based on wind direction categories for a daytime neutral case.

a)

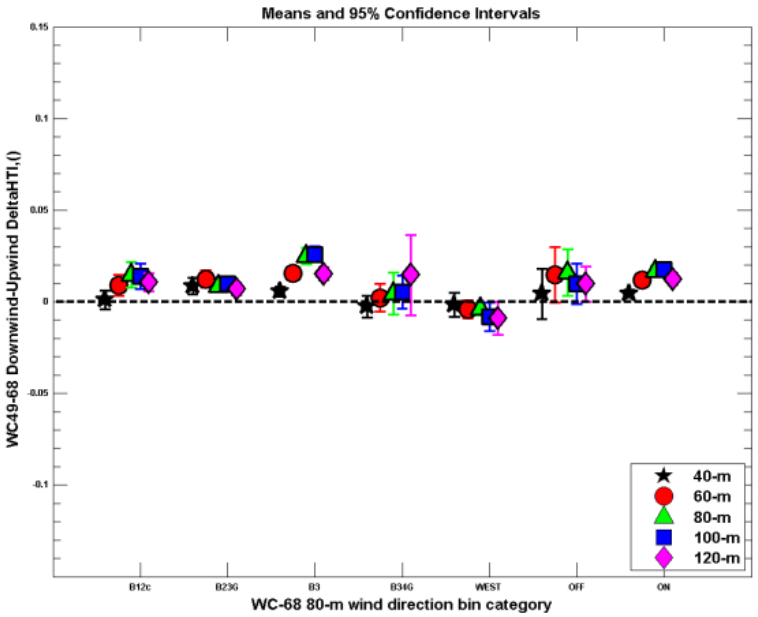

b)

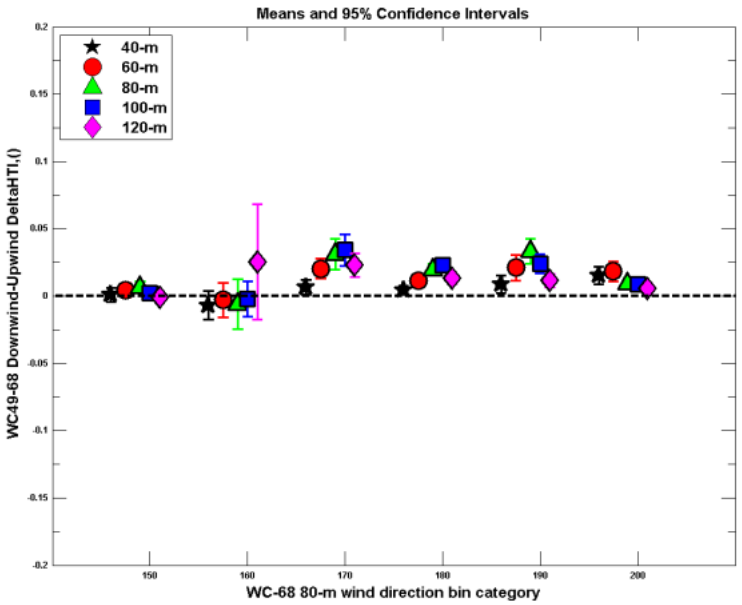

Fig. 6 a) and b) show means and 95% confidence intervals for ΔI_U based on wind direction categories for a nighttime stable case.

Height (m)	B3 vs. OFF N = 39 vs. 83		B3 vs. B12C N = 39 vs. 8		B3 vs. B23G N = 39 vs. 7		B23G vs. B34G N = 7 vs. 45		B3 vs. B34G N = 39 vs. 45	
	P-Value	$\overline{\Delta I_U}$	***P-Value***	$\overline{\Delta I_U}$	***P-Value***	$\overline{\Delta I_U}$	***P-Value***	$\overline{\Delta I_U}$	***P-Value***	$\overline{\Delta I_U}$
60	0.07	0.04	0.01	0.06	0.02	0.09	0.07	0.07	0.30	0.02
80	0.09	0.04	0.01	0.07	0.04	0.08	0.13	0.06	0.40	0.03
100	0.18	0.02	0.02	0.07	0.12	0.06	0.22	0.05	0.36	0.02

Table 2: Daytime unstable ΔI_U Two Sample Nonparametric Wilcoxon Method T-test ($\alpha = 0.05$) and ordered difference of directional bins B23 gapped flow vs. B34 gapped flow, B3 vs. OFF, B3 vs. B12 combo, B3 vs. B23 gapped flow, and B3 vs. B34 gapped flow from 60-100m.

Height (m)	B3 vs. OFF N = 92 vs. 1		B3 vs. B12C N = 92 vs. 35		B3 vs. B23G N = 92 vs. 18		B23G vs. B34G N = 18 vs. 63		B3 vs. B34G N = 92 vs. 63	
	P-Value	$\overline{\Delta I_U}$	***P-Value***	$\overline{\Delta I_U}$	***P-Value***	$\overline{\Delta I_U}$	***P-Value***	$\overline{\Delta I_U}$	***P-Value***	$\overline{\Delta I_U}$
60	0.31	0.04	**0.03**	**0.02**	0.26	0.01	0.12	0.02	0.58	0.002
80	0.36	0.03	**0.01**	**0.02**	0.07	0.02	0.10	0.02	0.87	0.002
100	0.36	0.03	**0.03**	**0.02**	0.02	0.03	0.06	0.02	0.68	0.003

Table 3: Daytime neutral ΔI_U Two Sample Nonparametric Wilcoxon Method T-test ($\alpha = 0.05$) and ordered difference of directional bins B23 gapped flow vs. B34 gapped flow, B3 vs. OFF, B3 vs. B12 combo, B3 vs. B23 gapped flow, and B3 vs. B34 gapped flow from 60-100m.

Height (m)	B3 vs. OFF N = 241 vs. 92		B3 vs. B12C N = 241 vs. 115		B3 vs. B23G N = 241 vs. 119		B23G vs. B34G N = 119 vs. 58		B3 vs. B34G N = 241 vs. 58	
	P-Value	$\overline{\Delta I_U}$	***P-Value***	$\overline{\Delta I_U}$	***P-Value***	$\overline{\Delta I_U}$	***P-Value***	$\overline{\Delta I_U}$	***P-Value***	$\overline{\Delta I_U}$
60	0.001	<0.001	0.001	0.01	0.001	0.003	0.08	0.01	<0.0001	0.013
80	<0.001	0.01	<0.001	0.01	**<.0001**	**0.02**	0.12	0.003	**<0.0001**	**0.020**
100	**<0.0001**	**0.02**	<0.001	0.01	**<.0001**	**0.02**	0.03	0.004	**<0.0001**	**0.021**

Table 4: Nighttime Stable ΔI_U Two Sample Nonparametric Wilcoxon Method T-test ($\alpha = 0.05$) and ordered differences of directional bins B23 gapped flow vs. B34 gapped flow, B3 vs. OFF, B3 vs. B12 combo, B3 vs. B23 gapped flow, and B3 vs. B34 gapped flow from 60-100m.